CASE REPORT

RJME
Romanian Journal of Morphology & Embryology
http://www.rjme.ro/

Morphology with immunohistochemical and genetic profiling of high-grade neuroendocrine carcinoma of colon – a case report with review of literature

ANDRZEJ WINCEWICZ[1)], ARTUR KOWALIK[2)], SEBASTIAN ZIĘBA[2)], STANISŁAW SUŁKOWSKI[3)], STANISŁAW GÓŹDŹ[4,5)]

[1)]*Non Public Health Care Unit, Department of Pathology (NZOZ Zakład Patologii Spółka z o.o.), Kielce, Poland*
[2)]*Department of Molecular Diagnostics, Holy Cross Cancer Centre, Kielce, Poland*
[3)]*Department of General Pathomorphology, Collegium Pathologicum, Medical University of Białystok, Poland*
[4)]*Department of Clinical Oncology, Holy Cross Cancer Centre, Kielce, Poland*
[5)]*Department of Prevention and Epidemiology of Neoplasms, Institute of Public Health, Faculty of Medicine and Health Sciences, Jan Kochanowski University, Poland*

Abstract

Here we present a challenging case of a hepatic flexure colon tumor of 61-year-old woman with no primary lesion of lung cancer. Immunohistochemistry was applied and 50 genes were analyzed by next-generation sequencing (NGS) technology. The tumor contained medium to large size neoplastic cells with evident nucleoli to be diagnosed poorly differentiated neuroendocrine predominantly large cell carcinoma of colon [G3: *World Health Organization* (WHO) 2010] (pT3 N0: 7th edition pTNM). Cytokeratin (CK) AE1/AE3 staining was predominantly membranous with partial distribution in "dot-like" pattern in perinecrotic cancer fields to be reminiscent of small cell carcinoma. Ki67 labeled over 90% of cancer cells with partial positive nuclear staining for thyroid transcription factor-1 (TTF-1). Using NGS, the following mutations were detected: nonsense mutations in four tumor suppressor genes [APC R1114X (molecular argument that the cancer was a primary tumor of colon), TP53 R213X, RB1 E137X and FBWX7 R393X & S282X], mutations in three receptor tyrosine kinases (RET A919V of high transforming activity, EGFR E114K and FLT3 L601I) well known as oncogenes.

Keywords: neuroendocrine tumors, colon, gene profiling, TTF-1, "dot-like" CK AE1/AE3 staining, APC R1114X.

Introduction

High-grade neuroendocrine carcinomas (HGNECs), notably small cell carcinomas of gastrointestinal tract, are extremely rare [1–3]. Incidence of colorectal neuroendocrine carcinomas is approximately 0.6% of all cancers at this location [2]. According to 2010 *World Health Organization (WHO) Classification* (with codes of *International Classification of Diseases for Oncology*, 3rd edition (ICD-O-3) given in brackets), there are the following histopathological types of neuroendocrine tumors (NETs) in the gastrointestinal and pancreatobiliary tracts: NET G1 (8240/3), NET G2 (8249/3) and neuroendocrine carcinoma (NEC) (8246/3), which include large cell NEC (8013/3) and small cell NEC (8041/3) [1, 4]. In this system, enterochromaffin cell (EC) cell serotonin-producing NET (8241/3) and mixed adenoneuroendocrine carcinoma (MANEC) 8244/3 are included as complete separate entities [1, 4]. NET G1 category is consistent with previously widely used carcinoid category [1, 4]. However, 2010 *WHO Classification* still contains tumors with preserved carcinoid term in the nomenclature: goblet cell carcinoid (8241/3) and tubular carcinoid (8245/1) that are found in appendix and extrahepatic bile duct (8245/1). In addition, L cell, glucagon-like peptide and pancreatic polypeptide/peptide YY (PP/PYY)-producing NETs grow in small intestine, appendix, colorectum (8152/1), while somatostatin-producing NET (somatostatinoma) occurs in ampulla of Vater, small intestine, pancreas (8156/3) and gastrin-producing NET (gastrinoma) (8153/3) limits its occurrence to stomach, ampulla, small intestine, pancreas [1, 4]. On the other hand, glucagon-producing NET (glucagonoma), insulin-producing NET (insulinoma) (pancreas – 8151/3), vasoactive intestinal peptide (VIP)oma (pancreas – 8155/3), neuroendocrine microadenoma (8150/0) are typical pancreatic tumors (8152/3) [1, 4]. On the other pole of *WHO Classification*, due to its peculiar morphological distinctness, gangliocytic paraganglioma remains to grow in ampulla of Vater and small intestine (8683/0) [1, 4].

The clinical picture of HGNECs presents local high aggressiveness and rapid dissemination, usually presenting with nodal and distant organ metastases [5]. HGNECs usually grow in the right colon with advanced pTNM stage at diagnosis, usually designated not less than pT3 with frequent involvement of tunica serosa and extension beyond intestinal wall justifying pT4 designation [1]. Rapidness of growth may be so exaggerated that HGNECs of colon could present as emergency cases similarly to conventional adenocarcinoma due to rupture of tumor [6, 7]. Namely, MANEC was reported to undergo rupture of one hepatic metastatic tumor after surgical removal of

primary a high-grade large cell neuroendocrine carcinoma (LCNEC) that contained also texture of differentiated tubular adenocarcinoma [8]. In a study of reasonably large number of consecutive 100 colorectal HGNECs from *MD Anderson Cancer Center*, increased levels of lactate dehydrogenase predicted a worse outcome [9]. In this survey, up to 89% of cancers were diagnosed small cell carcinoma and metastatic spread was present in 64% cases at the time of diagnosis with median overall survival (OS) equaling 14.7 months, resulting in the rate of 8% in case of five-year-long OS [9]. In the largest analyzed so far group of 1367 colorectal NECs, it was found that better median, 21 month-long, OS was associated with surgical removal of localized non-small-cell NEC, in comparison to 6-month-long median survival for surgery spared patients[10]. Similarly, in another study of 81 colon and 526 rectal NETs, which included 578 G1 NETs, 17 G2 NETs and 12 NECs, the median OS was 19.3 months in 22 metastatic NETs and the most common metastatic site was liver [11]. Indeed, the course of the disease is so severe and fatal [5] that multiple therapies are considered to reverse ominous prognosis, *e.g.*, mammalian target of rapamycin (mTOR) inhibitor everolimus was shown to significantly diminish proliferation of these highly mitotically active neoplasm in preclinical experimental models of poorly differentiated neuroendocrine carcinomas (PDNECs) that are characterized by strong expression of mTOR pathway components [5]. Such a therapy is encouraged as a standard treatment at least in pancreatic tumors [12]. Japanese classification of colorectal cancers distinguishes endocrine cell carcinoma category, which incorporates two entities of 2010 *WHO Classification*: NEC and MANEC [6]. According to Komatsubara *et al.*, most reviewed, endocrine cell carcinomas of the colon and rectum were MANECs [6]. Small cell NEC could obstruct anal canal with clinical symptoms of constipation [7]. HGNECs have predilection for sigmoid or the anorectal regions, with the most common rectal location [9]. Incidentally, NECs could arise in the retrorectal space, with one report of 8 cm in diameter tumor adjacent to lower rectum that was consisted of cystic texture of high- and low-grade components of 53-year-old woman [13]. In its rarity, small cell carcinoma could be sporadic but it was also reported to arise in association with Lynch syndrome [14]. Biology and clinics of HGNECs could be reminiscent of pulmonary NECs, as one rectal small-cell neuroendocrine carcinoma of a 68-year-old woman presented with hyponatremia due to abnormal levels of vasopressin and developed the paraneoplastic syndrome of inappropriate antidiuretic hormone (SIADH) secretion that responded to vasopressin antagonists [15]. Recently, 14 of metastatic gastroenteropancreatic NETs of pancreas, small intestine, ascending colon, distal colon and rectum [gastroentero-pancreatic (GEP)-NET] (eight NECs and six NETs) underwent molecular profiling with appliance of Ion AmpliSeq Cancer Hotspot Panel v2 to screen structure of 50 commonly mutated genes to detect most frequently mutations of *SMARCB1*, *TP53*, *STK11*, *RET* and *BRAF* genes [16].

Due to rarity of colon neuroendocrine carcinomas, we aimed to report the case of 61-year-old woman with gene profiling of her colon cancer.

Case presentation

Here we present a neuroendocrine carcinoma of 61-year-old female patient admitted to hospital with intestinal obstruction due to intestinal tumor of hepatic flexure of colon. The initial clinical symptoms included non-specific blunt pain in the right side lower abdominal area. The color of stool was variable. Namely, it was dark, brown or mixed with blood. Additional tests revealed hypochromic anemia blood in stool with no reported heredo-collateral history of colorectal cancer in her close relatives nor any environmental hazards in her life and work conditions that would be conclusive for this case.

Preoperatory cTNM staging was not reported as the patient urgently underwent surgical operation due to intestinal obstruction. The surgical intervention was open right hemicolectomy (ORH) that comprised surgical resection of part of terminal ileum, the cecum, the ascending colon, the hepatic flexure with small part of the transverse colon, together with peri-intestinal fat and regional lymph nodes [17]. The patient underwent post-operative adjuvant therapy and passed away in one year from initial diagnosis due to dissemination of neoplastic disease.

The postoperative material was fixed in 10% buffered formalin solution (4% formaldehyde solution) for 72 hours. The surgical removal included 9 cm long terminal part of ileum, and 16 cm long right-sided part of large intestine with vermiform appendix of length of 4 cm and diameter of 0.5 cm with part of omentum measuring 20×11×1cm. Clinically and on macroscopic pathological evaluation, ulcerated, slightly depressed, 5 cm in diameter, fleshy white tumor of endophytic type was present in colon in a distance of 8 cm from resection line of the surgical distal margin. The cancer was hardened, ulcerative, infiltrative, endophytic and annular, whitish on transaction and covered with red-brown cap on ulcerated surface. On the transection tumor infiltrated through the full thickness of tunica muscularis propria and beyond approximating the full thickness of the intestinal wall. The histological structures like ganglions and lymphatic vessels were not invaded in adjacent areas to cancer infiltrate and there was no residual normal histological formation inside destructive growth of the malignancy in obtained microscopic samples. Tumor infiltrated tunica mucosa, submucosa and muscularis propria of large intestine into subserosal tissue of colon. The tumor did not invaded the peritoneal surface as there was no ulceration of peritoneal surface nor evident penetration of mesothelial layer by malignant cells. Representative samples were collected, sampled and stained with mucicarmine, synaptophysin, chromogranin, cytokeratin (CK) AE1/AE3, Ki67, thyroid transcription factor-1 (TTF-1), CK 20 and alpha-fetoprotein (AFP). The thickness of microscopic sections was 5 μm, the slides underwent deparaffinization, clarification, and hydration with blockage of endogenous

peroxidase with 5% hydrogen peroxide for 10 minutes. Following primary antibodies were applied: Novocastra™ liquid mouse monoclonal antibody NCL-SYNAP-299 [clone 27G12 SYNAP-299-L-CE, 1 mL NCL-L-SYNAP-299, liquid concentrated monoclonal antibody Novocastra, 1:100 dilution, incubation time for 60 minutes, at 25^0C, after high temperature antigen retrieval using 0.01 M citrate retrieval solution (pH 6), Novocastra], lyophilized mouse monoclonal IgG1 antibody chromogranin A (product code: NCL-CHROM-430, clone 5H7, 1:200 dilution, 60 minutes primary antibody incubation, at 25^0C, after high temperature antigen retrieval, standard ABC (avidin-biotin complex) technique, Leica Biosystems Newcastle Ltd., UK), Novocastra™ liquid mouse monoclonal IgG1 antibody thyroid transcription factor-1 [product code: NCL-L-TTF-1, clone SPT24 human thyroid transcription factor-1 (TTF-1), 1:200 dilution, for 30 minutes, at 25^0C], Novocastra™ liquid mouse monoclonal IgG2a, kappa antibody cytokeratin 20 (product code: NCL-L-CK20, clone Ks20.8, 1:50 dilution, for 30 minutes, at 25^0C, Novocastra Epitope Retrieval Solution, pH 6), Bond™ ready-to-use primary (RTU) antibody, Ki67 (K2) catalog No. PA0230, monoclonal mouse anti-human cytokeratin [clone AE1/AE3, isotype IgG1, kappa, code M3515, 1:50 dilution, LSAB2 (labeled streptavidin–biotin peroxidase kit)], FLEX polyclonal rabbit anti-human alpha-1-feto-protein (Dako Denmark, Glostrup, Denmark). In case of Novocastra antibodies, retrieval solution was 0.01 M citrate buffer (pH 6) that was heated until boiling point for 5 minutes kept later in operating temperature for one minute in a stainless steel pressure cooker with the lid in recommended quantity of 1500 mL. Alter exposure to unmasking solution, the slides were placed in bath of tap water, followed by washing in Tris-buffered saline (TBS) buffer (pH 7.6) for 1×5 minutes and immersing the sections in diluted normal serum (or RTU normal horse serum) for 10 minutes and later entering incubation with exact primary antibody in time specified for each antibody. TBS buffer solution was subsequently used for washing of the slides 2×5 minutes. Where ABC visualization technique was recommended for appliance, slides were incubated slides in ABC reagent or RTU streptavidin/peroxidase complex and with interval TBS washing incubated with in 3,3'-diaminobenzidine (DAB) for 5 minutes.

Tumor infiltrated tunica mucosa, submucosa and muscularis propria of large intestine. Twenty-five local lymph nodes were isolated from postoperative material and evaluated in Hematoxylin–Eosin (HE) and CK AE1/AE3 staining. The cancer contained predominantly solid growth pattern, on careful inspection reminiscent of syncytia, trabeculae and focally slit like arrangements resembling residual gland like formation. Infiltrative front of the tumor consisted of tongues or solid fields of undifferentiated cancer cells that dispersed into small groups, which intersected with invaded non-neoplastic stroma of connective tissue. Thus, the front of tumor invasion certainly was not pushing border: it was apparently dispersive as in primary high-grade neuroendocrine cancers of lungs and other non-intestinal sites. Thus, designation of the way of local invasion of this peculiar tumor as tumor budding was discouraged in our opinion as it is not conventional adenocarcinoma of colon *in toto* or even in a small representative part to assess budding feature. The number of mitoses exceeded 70 in 10 high-power fields (HPFs: ×400 microscopic field). The tumor cellularity was high as the cancer cells were densely packed with overlapping one over another. Tumor necrosis exceeded 10% of surface of microscopically evaluated tumor samples but it was less than 50% of total cancer texture. There were areas of hemorrhages. Any adjacent structures like blood and lymphatic vessels were not visible in microscopic tumor samples due to widespread invasion. In sampled tissues, there were no ganglion structures or nerves to be infiltrated with cancer. Apparently, tumor growth was so destructive, that it did not spare such structures within the tumor.

The neoplastic cells were medium to large size and their nuclei had coarse chromatin and evident nucleoli (Figure 1).

The cancer texture constituted poorly differentiated appearance with predominant undifferentiated areas but focally showing some of adenocarcinoma features but it was much less than 30% to designate the tumor as MANEC. Mucicarmine was negative in tumor tissues. It was diagnosed poorly differentiated neuroendocrine predominantly LCNEC (category G3: *WHO* 2010) (pT3 N0: 7^{th} edition pTNM). Ki67 labeled much over 90% of nuclei of malignant cells (Figure 2d). CK AE1/AE3 was predominantly membranous (Figure 2b) with partial distribution in "dot-like" pattern in perinecrotic cancer fields to be reminiscent of small cell carcinoma of lung counterpart in over 90% of malignant cells (Figure 2, a and c). CK 20 was negative (Figure 3b), while AFP gave a shadow of positivity with limited reliability of obtained result of staining in much less than 5% of cancer cell population (Figure 3a). There was partial positive nuclear staining for TTF-1 (Figure 3c). Synaptophysin was strongly positive in cytoplasm of cancer tissues in granular manner in over 70% of malignant cells (Figure 3d). Due to current guidelines that recommend using a couple of neuroendocrine (NE) markers, such as chromogranin A and synaptophysin, finally chromogranin staining was preformed with weak microgranular and partly diffuse but apparently positive result in up to 50% malignant cells (Figure 4.). Anyway, synaptophysin positivity and apparent HE neuroendocrine appearance served as sufficient ground to state neuroendocrine nature of the lesion. Our case is at least partially a small cell carcinoma as the CK AE1/AE3 does show some "dot-like" pattern in part of our tumor. However, predominantly large neoplastic cell equipped with evident nucleolus was diagnostic enough to favor diagnosis of large cell neuroendocrine carcinoma over small cell carcinoma in main component. Taking into account a great dynamics of growth of primary tumor (over 90% positive cancer cells for nuclear staining of Ki67), it was a bit surprising not to reveal any lymph nodal metastases in HE staining nor any keratin positive deposits of cancer cells in verifying CK AE1/AE3 labeling of 25 sampled lymph nodes. The percentage of Ki67-positive neoplastic cells

was counted manually of at least 500 cells in "hot spots" during routine microscopic reviewing of immunohistochemically-stained slides and later repeated on printed photographic images of hot spots [18]. The patient gave her informed consent for medical procedures, which are presented in this case report without any identifying personal details of the patient. CDX2 a maker of gastrointestinal origin was considered to be included in the immunohistochemical panel, but instead of it we decided to perform more reliable and sensitive genetic testing of next generation sequencing to reveal molecular signatures of the tumor in the most possible reliable way.

For genomic study, DNA was isolated from formalin-fixed paraffin-embedded (FFPE) tissue samples from area marked by pathologist on HE slides. Namely, unstained slides were positioned on HE slide with marked area of tumor cells in order to mark area for macrodissection on unstained slides. After macrodissection, DNA was isolated using Maxwell 16 device (Promega, USA) (the cancer tissue which was dissected was mainly of neuroendocrine poorly differentiated nature, the tubular component was sparse much less below 5% of neoplastic texture; actually, samples for molecular analysis contained almost exclusively densely packed texture of neuroendocrine carcinoma with only some peritumoral tissue on the periphery of the sample). The concentration of isolated DNA assessed by Qubit fluorometer 2.0 according to manufacturers instruction (Thermo Fisher Scientific, USA).

The concentration of isolated DNA was at the level of 30 ng/μL, which was enough to start library preparation for NGS. The final quality check of quality of isolated DNA was at step of the library dilution factor quantification by quantitative polymerase chain reaction (qPCR) technique just before emulsion PCR step.

Next generation sequencing (NGS) was performed to analyze 50 the most often mutated oncogenes and tumor suppressors (Ion AmpliSeq™ Cancer Hotspot Panel v2, Thermo Fisher Scientific, USA). The status of following genes were investigated: ABL1 (Abelson murine leukemia viral oncogene homolog 1), EZH2 (Enhancer of zeste homolog 2), JAK2 (Janus kinase 2), JAK3 (Janus kinase 3), PTEN (Phosphatase and tensin homolog), AKT1 (serine–threonine specific protein kinase AKT–PKB), FBXW7 (F-box and WD40 repeat domain-containing 7), IDH1 (isocitrate dehydrogenase 1), IDH2 (isocitrate dehydrogenase 2), PTPN11 (tyrosine-protein phosphatase non-receptor type 11), ALK (anaplastic lymphoma kinase), FGFR1 (fibroblast growth factor receptor 1), KDR (kinase insert domain receptor), RB1 (retinoblastoma 1 gene), APC (adenomatous polyposis coli), FGFR2 (fibroblast growth factor receptor 2), KIT, RET (rearranged during transfection receptor tyrosine kinase), ATM (ataxia-telangiectasia mutated), FGFR3 (fibroblast growth factor receptor 3), KRAS (V-Ki-ras2 Kirsten rat sarcoma viral oncogene homolog), SMAD4 [SMAD family member 4: (MAD) from homolog of mothers against decapentaplegic and (S) from the *Caenorhabditis elegans* protein SMA (from gene *sma* for small body size)], BRAF (proto-oncogene B-Raf), FLT3 (Fms like tyrosine kinase 3), MET (MET proto-oncogene), SMARCB1 (SWI/SNF-related matrix-associated actin-dependent regulator of chromatin subfamily B member 1), CDH1 (cadherin-1), GNA11 (guanine nucleotide-binding protein subunit alpha-11), MLH1 (MutL homolog 1), SMO (smoothened, frizzled class receptor), CDKN2A (cyclin-dependent kinase inhibitor 2A), GNAS (guanine nucleotide binding protein, alpha stimulating), MPL (myeloproliferative leukemia virus oncogene), SRC (proto-oncogene tyrosine-protein kinase Src sarcoma Rous), CSF1R (colony stimulating factor 1 receptor), GNAQ [guanine nucleotide-binding protein G(q)], NOTCH1 (Notch homolog 1, translocation-associated), STK11 (serine/threonine kinase 11), CTNNB1 (catenin beta 1), HNF1A (hepatocyte nuclear factor 1 homeobox A), NPM1 (nucleophosmin1 gene), TP53 (tumor protein p53), EGFR (epidermal growth factor receptor), HRAS (GTPase HRas: transforming protein p21), NRAS (N-Ras), VHL (von Hippel–Lindau tumor suppressor), ERBB2 [receptor tyrosine-protein kinase erbB-2: proto-oncogene ERBB2; ERBB2 gene encodes HER2 (human epidermal growth factor receptor 2) – HER2/neu], ERBB4 (Erb-B2 receptor tyrosine kinase 4), platelet-derived growth factor receptor alpha (PDGFRA), PIK3CA (phosphatidylinositol-4,5-bisphosphate 3-kinase, catalytic subunit alpha) (Table 1).

NGS was performed using and Personal Genome Machine, Ion Torrent, Thermo Fisher Scientific, USA.

Table 1 – ***NGS results for HGNEC of colon***

Gene ID	Position	AA change	Coverage	Frequency [%]	TS VC	CLC	Galaxy
RET	43617419 C>T	A919V	1244	36	+	+	+
APC	112174631 C>T	R1114X	1924	34	+	+	+
TP53	7578212 G>A	R213X	921	57	+	+	+
EGFR	55211097 G>A	E114K	1211	36	+	+	
FBXW7	153250883 G>A	R393X	683	30	+	+	+
FBXW7	153258970 G>T	S282X	1133	36	+	+	+
FLT3	28608255 G>T	L601I	915	29	+	+	+
RB1	48919244 G>T	E137X	457	31	+	+	+

NGS: Next generation sequencing; HGNEC: High-grade neuroendocrine carcinoma; Position: According to hg19; AA: Amino acid; Coverage: Number of times the site of mutation was sequenced; Frequency: Rate of particular mutation detected in the sample. Name of the softwares used for NGS data analysis: TSVC – TORRENT SERVER VARIANT CALLER – calls single-nucleotide polymorphisms (SNPs), multi-nucleotide polymorphisms (MNPs), insertions, and deletions in a sample across a reference or within a targeted subset of that reference. Software embedded in torrent server; CLC: CLC Genomic Workbench NGS v9 – data analysis software from Qiagen Company; Galaxy is an open source, web-based platform for data intensive biomedical research (https://usegalaxy.org/).

The analysis of NGS data was performed using three different programs to cross validate the results. The raw data generated during sequencing was processed and aligned (mapped) to the reference sequence of the human genome (hg19) with the Torrent Server Suite 4.2. Variant calling was performed by Variant Caller v4.2 embedded in the Torrent Server Suite 4.2. with default parameters. Detected variants were viewed by the Integrative Genomics Viewer. The raw data were also analyzed by the CLC Genomics Workbench program 7.5.1 (QIAGEN) and GALAXY platform (www.usegalaxy.org). Called variants by the Torrent Server Suite 4.2 and the GALAXY was annotated with the wANNOVAR tool (http://wannovar.wglab.org/).

The following mutations were detected: nonsense single nucleotide mutations in four tumor suppressor genes [APC R1114X (molecular argument that the cancer was a primary tumor of colon), TP53 R213X, RB1 E137X and FBWX7 R393X & S282X], which caused premature stop codon creation and the protein truncation (Figure 4, Table 1). We also detected single nucleotide mutations in three receptor tyrosine kinases (RET A919V, EGFR E114K and FLT3 L601I) well known as oncogenes (Table 1, Figure 6). NGS results were robust enough to be not validated by using Sanger sequencing (Table 1, Figures 5 and 6). Particularly, we did not perform Sanger validation because frequency of detected mutation is high enough as depicted in the table, reviewing detected traces by using Integrative Genomics (IGV) Viewer we saw proper balance between DNA strands (in other words mutation was present on both strands) and there is no big homopolymer stretches in close proximity of mutation. Moreover, to assure the highest level of reliability sequencing data were analyzed by three softwares for cross validation. In accordance of vendor, "SNP detection sensitivity – 98% detection rate for 5% variant frequency at positions with average sequencing coverage from 1,000X to 4,000X" coverage of detected mutation was between 457X–1924X and alleles frequencies was between 29–57%, so it means that the coverage was enough to call variants with very high confidence. Thus, we added information about coverage to the Table 1.

We did not perform validation status of detected mutation (somatic *vs.* inherited) because all of them have been already described in COSMIC (Catalogue Of Somatic Mutations In Cancer) database and we had limited funding.

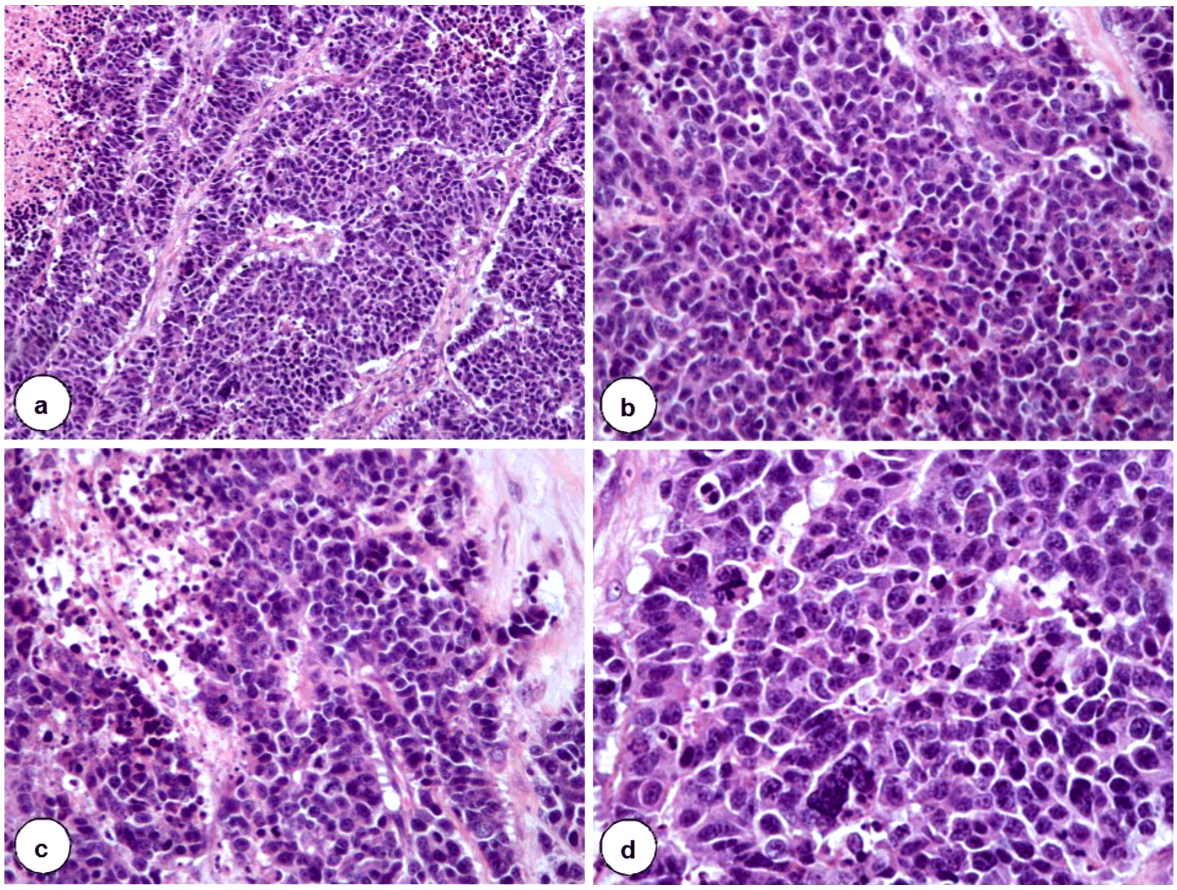

Figure 1 – ***Morphology of large cell neuroendocrine carcinoma (LCNEC) in HE staining: (A) Sheets of high-grade malignancy with somewhat trabecular pattern (×200); (B and C) Focal necrosis in nested and trabecular areas of the cancer (×400); (D) Neuroendocrine, "salt and pepper" chromatin distribution of nuclei of cancer cells – cellular pleomorphism and atypical mitoses in the malignant texture (×600).***

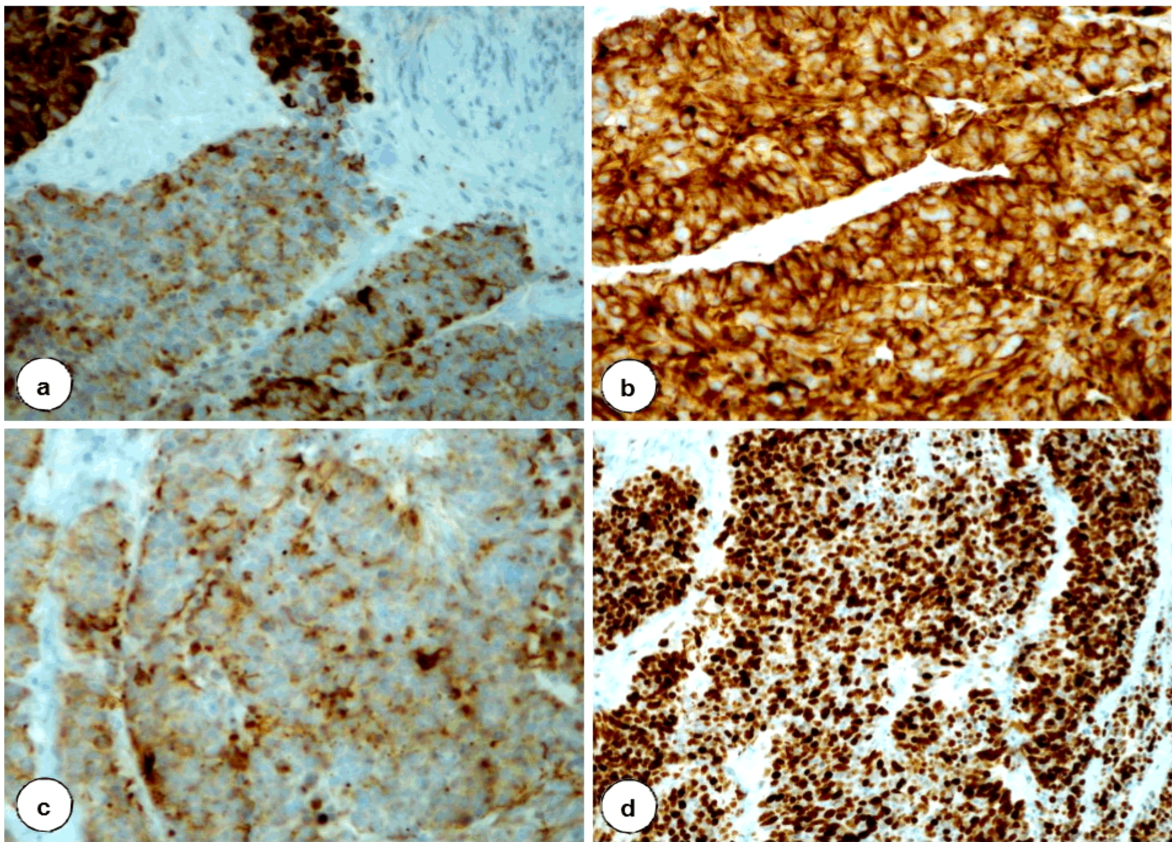

Figure 2 – ***Immunohistochemistry of LCNEC: (A and C) Partial distribution CK AE1/AE3 staining in "dot-like" pattern in perinecrotic cancer fields to be reminiscent of small cell carcinoma of lung counterpart (×400); (B) Membranous and cytoplasmic distribution of CK AE1/AE3 in carcinomatous texture (×400); (D) Intense nuclear staining for Ki67 in majority of nuclei of malignant cells (×400).***

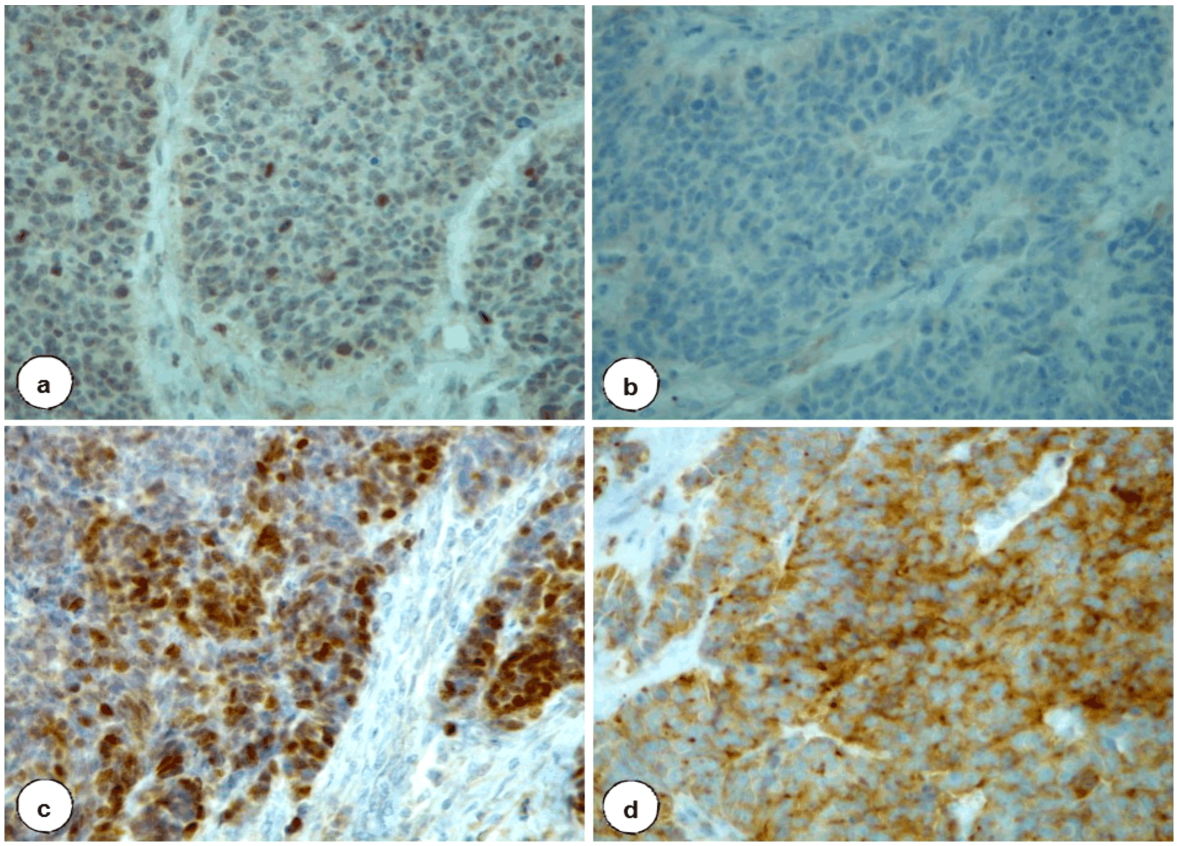

Figure 3 – ***Immunohistochemistry of LCNEC: (A) A shadow of positivity with limited reliability of obtained result of staining for AFP (×400); (B) Negative staining for CK 20 in carcinomatous fields (×400); (C) A partial positive nuclear staining for TTF-1 (×400); (D) Cytoplasmic positivity to synaptophysin in cancer tissues (×400).***

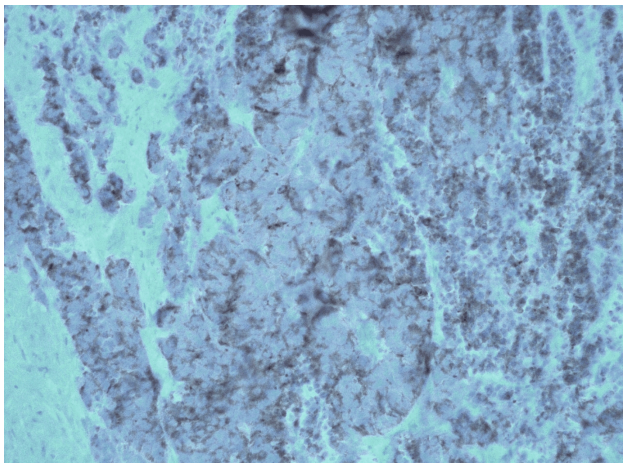

Figure 4 – ***Immunohistochemistry of LCNEC: Weak cytoplasmic positivity to chromogranin A in cancer population (×200).***

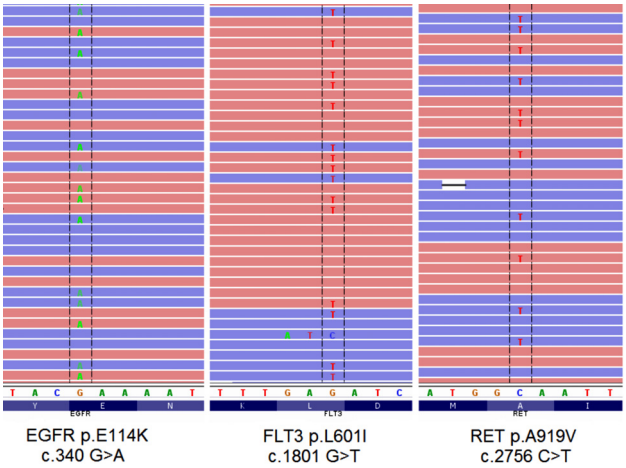

Figure 5 – ***Nonsense mutations detected in four tumor suppressor genes [APC R1114X, TP53 R213X, RB1 E137X and FBWX7 R393X & S282X], NGS data showing reads (- strand designated in blue, + strand in red) mapped to the tumor suppressor genes reference sequences shown below the panel box depicted by Integrative Genomics Viewer.***

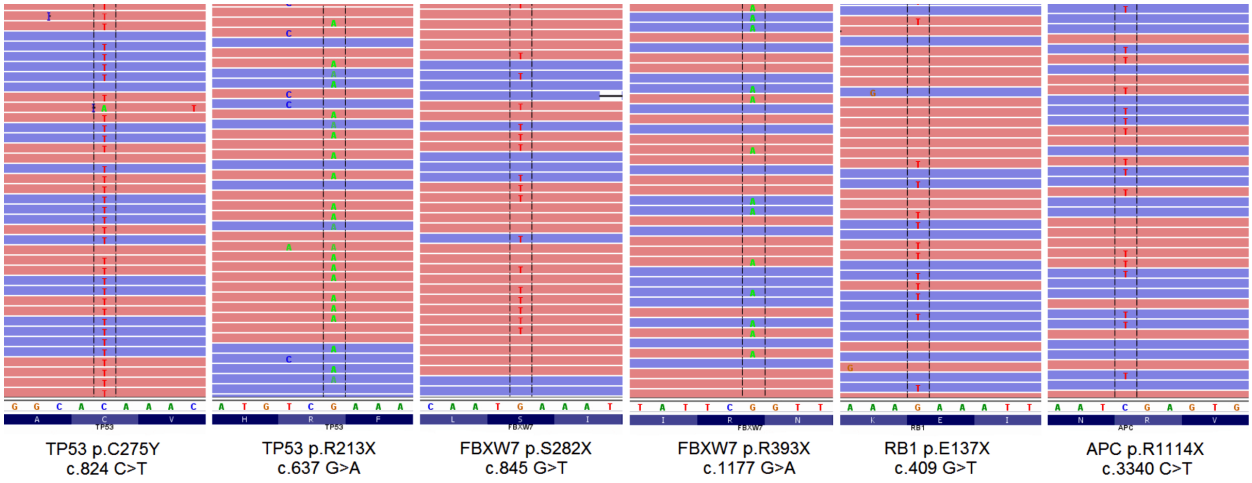

Figure 6 – ***Missense mutations detected in three oncogenes [RET A919V, EGFR E114K and FLT3 L601I], NGS data showing reads (- strand designated in blue, + strand in red) mapped to the oncogenes reference sequences shown below the panel box depicted by Integrative Genomics Viewer.***

Discussion

In our reported case, most of cancer texture contained malignant cells that exceeded much over three times the size of lymphocyte and most of these cells had discernible and pronounced nucleoli. In contact to small cell carcinoma, large cell neuroendocrine carcinoma contains nesting, "rosette-like" organoid, trabecular, and palisading texture of relatively large cells with more abundant cytoplasm and prominent nucleoli with more vesicular pattern of nuclear chromatin [1, 19]. The trabecular pattern was the most striking architectural feature of our reported tumor. However, the criterion of cell size less than three lymphocytes is not absolute in minority of small cell carcinoma cases, whose malignant cells could be of size up to 6–7 lymphocytes with some morphometric studies that found larger malignant cell size (exceeding three times the diameter of a lymphocyte) in 30% of analyzed small cell lung carcinomas [19]. Thus, in differential diagnosis with LCNEC due to variety of cell size, additional cytological criteria are diagnostic for small cell lung carcinoma (SCLC), such as finely granular chromatin, lack of prominent nucleoli, lack of prominent cell borders [19]. In our case, the diagnosis of small cell carcinoma was considered as there was a minor rate of smaller cells with indistinct cell borders and lack of nucleoli with dusty chromatin pattern within "dot-like" pattern of CK AE1/AE3 staining [1]. Our tumor morphology and its immunoprofile recapitulate some of features of NEC of pulmonary counterpart in our case. TTF-1 positivity rendered us to exclude any focal pulmonary lesion. The positive TTF-1 staining is of great interest here and was worrisome as there was no lung lesion to make as think about colon tumor as metastasis of pulmonary primary cancer. However, TTF-1 positivity could be seen in primary extrapulmonary small cell carcinoma [20]. Namely, even primary tumor of ureter was reported to present with small cell NEC morphology and to express TTF-1 in a case of 71-year-old man [20]. In our differential diagnosis of large *versus* small cell carcinoma, we relied on widely recognized criteria that malignant cells are three times larger than a lymphocyte to classify them as

cells of LCNEC in opposition to small cell carcinoma in lung tumors [19].

As reported above, our tumor focally presented some of adenocarcinoma features in a quantity less than 30% criterion of qualifying a neoplasm into MANEC category. Anyway, the differential diagnosis of our tumor naturally included MANEC due to possible occurrence of combined neoplasms in case of primary combined NEC (small-cell type) and squamous cell carcinoma or mucinous adenocarcinoma and NEC [21, 22]. There is no standard panel of immunohistochemical stainings in HGNEC, but we believe that a broad spectrum of immunohistochemical stainings should be applied as in case of MANEC of 68-year-old woman [23]. Our tumor showed similar mutational status to that one that was reported by Vanacker *et al.* in MANEC, which harbored somatic mutations in APC, Kirsten rat sarcoma viral oncogene homolog (KRAS), B-cell chronic lymphocytic leukemia (CLL)/lymphoma 9 (BCL9) and Forkhead Box P1 (FOXP1) as well exclusive for neuroendocrine component mutation in SWI/SNF related, matrix-associated, actin-dependent regulator of chromatin, subfamily a, member 4 (SMARCA4) of potential properties that would drive transformation of conventional adenocarcinoma into the neuroendocrine component [24]. Synchronicity of small cell neuroendocrine carcinoma and adenocarcinoma rendered even suspicion of common stem cell origin that aggravated with observations of relatively frequent coincidence of conventional adenocarcinoma with rare small cell carcinomas in gastrointestinal tract [25].

As molecular proof of being a primary cancer of large bowel, our tumor presented with nonsense mutation APC R1114X that results in a premature stop codon. Mutation in *APC* occurs at early stages of colorectal carcinogenesis process [26, 27]. This mutation was described as a germline and somatic as well. Although the presence of *APC* mutation is not tautologically related to large bowel adenocarcinoma, because it is common to carcinomas elsewhere, the germline mutation of this kind predisposes to familial APC syndrome [27, 28]. However, it is important to note that our tumor did not clinically occur in familial adenomatous polyposis (FAP) syndrome. Moreover, high-grade NEC is extraordinary rare in patients with FAP to note a case of a 60-year-old man with FAP with regional lymph node and liver metastatic involvement [29]. We were also able to detect TP53 R213X nonsense mutation, which was already described in colorectal cancer (CRC) sample [28]. It should be noted that studies on cancer cell lines carrying TP53 R213X mutation revealed the possible way of restoration of re-expression of full length TP53 by aminoglycoside antibiotics (gentamicin), which can bind to mammalian ribosome and promote stop codon read through partially inducing full-length protein synthesis [30]. We also detected E114K mutation in *EGFR* gene. This mutation has been already described in CRC cancer [27]. Another tumor suppressor, which we found mutated was FBXW7. We detected two nonsense mutations S282X and R393X of this gene. These two mutations have been already described in CRC, but never in the same tumor. Unfortunately, we were not able to reveal, whether these mutation are on the same alleles, different alleles or different cell clones. One of the FBXW7 mutations (R393X) was already detected in coexistence with R213X APC mutation [31]. In the present work, we have detected similar association of FBWX7 R393X with APC R1114X mutation. It should be noticed that mutation in *FBXW7* gene acts in cooperation with *TP53* mutation marking progression from adenoma to carcinoma in animal model. Furthermore, due to eventual therapeutic implications it is worth mentioning, that mutated or lost of *FBWX7* in HTC116 cancer cell line induced resistance to oxaliplatin [32]. The next revealed mutation in our tumor is RET A919V that was previously described in sporadic medullary thyroid carcinoma and found to possess high transforming activity [33, 34].

To our knowledge, our present report is the first report of FLT3 L601I mutation in NEC of colon. In this aspect, it is worth mentioning that two mutations L601F and L601P are present in the COSMIC database, wherein L601P mutation was detected in metastatic cutaneous squamous cell carcinoma [35]. We also detected RB1 E137X non-sense mutation, which has been already described in CRC cell line [36]. Here, it should be noted that TP53 and RB1 mutations are akin to a *de novo* NEC.

In summary, our molecular study has revealed nonsense mutation in four tumor suppressor genes (*APC*, *TP53*, *RB1* and *FBWX7*). *TP53* and *RB1* are regarded as most important genes regulating cell cycle, while *APC*, *TP53* and *FBXW7* are implicated in tumor progression from adenoma to carcinoma.

Conclusions

Our report is the first in the literature to report such a set of gene mutations based on NGS analysis in poorly differentiated neuroendocrine carcinoma of colon among scarcity of similar studies of neuroendocrine tumors of alimentary tract.

Conflict of interests

The authors declare that they have no conflict of interests.

References

[1] Bosman FT, Carneiro F, Hruban RH, Theise ND (eds). World Health Organization (WHO) Classification of Tumours of the Digestive System. 4th edition, International Agency for Research on Cancer (IARC) Press, Lyon, France, 2010, 1–418.

[2] Bernick PE, Klimstra DS, Shia J, Minsky B, Saltz L, Shi W, Thaler H, Guillem J, Paty P, Cohen AM, Wong WD. Neuroendocrine carcinomas of the colon and rectum. Dis Colon Rectum, 2004, 47(2):163–169.

[3] Gaffey MJ, Mills SE, Lack EE. Neuroendocrine carcinoma of the colon and rectum. A clinicopathologic, ultrastructural, and immunohistochemical study of 24 cases. Am J Surg Pathol, 1990, 14(11):1010–1023.

[4] Kim JY, Hong SM. Recent updates on neuroendocrine tumors from the gastrointestinal and pancreatobiliary tracts. Arch Pathol Lab Med, 2016, 140(5):437–448.

[5] Bollard J, Couderc C, Blanc M, Poncet G, Lepinasse F, Hervieu V, Gouysse G, Ferraro-Peyret C, Benslama N, Walter T, Scoazec JY, Roche C. Antitumor effect of everolimus in preclinical models of high-grade gastroenteropancreatic neuroendocrine carcinomas. Neuroendocrinology, 2013, 97(4): 331–340.

[6] Komatsubara T, Koinuma K, Miyakura Y, Horie H, Morimoto M, Ito H, Lefor AK, Sata N, Fukushima N. Endocrine cell carcinomas of the colon and rectum: a clinicopathological evaluation. Clin J Gastroenterol, 2016, 9(1):1–6.

[7] Lee RT, Ferreira J, Friedman K, Moss SF. A rare cause of constipation: obstructing small cell neuroendocrine carcinoma of the anal canal. Int J Colorectal Dis, 2015, 30(9):1291–1292.

[8] Ito H, Kudo A, Matsumura S, Ban D, Irie T, Ochiai T, Nakamura N, Tanaka S, Tanabe M. Mixed adenoneuroendocrine carcinoma of the colon progressed rapidly after hepatic rupture: report of a case. Int Surg, 2014, 99(1):40–44.
[9] Conte B, George B, Overman M, Estrella J, Jiang ZQ, Mehrvarz Sarshekeh A, Ferrarotto R, Hoff PM, Rashid A, Yao JC, Kopetz S, Dasari A. High-grade neuroendocrine colorectal carcinomas: a retrospective study of 100 patients. Clin Colorectal Cancer, 2016, 15(2):e1–e7.
[10] Shafqat H, Ali S, Salhab M, Olszewski AJ. Survival of patients with neuroendocrine carcinoma of the colon and rectum: a population-based analysis. Dis Colon Rectum, 2015, 58(3): 294–303.
[11] Kim ST, Ha SY, Lee J, Hong SN, Chang DK, Kim YH, Park YA, Huh JW, Cho YB, Yun SH, Lee WY, Kim HC, Park YS. The clinicopathologic features and treatment of 607 hindgut neuroendocrine tumor (NET) patients at a single institution. Medicine (Baltimore), 2016, 95(19):e3534.
[12] Weber HC. Medical treatment of neuroendocrine tumours. Curr Opin Endocrinol Diabetes Obes, 2013, 20(1):27–31.
[13] Misawa S, Horie H, Yamaguchi T, Kobayashi S, Kumano H, Lefor AT, Yasuda Y. A unique retrorectal tumor with neuroendocrine differentiation: case report and review of the literature. Int J Surg Pathol, 2013, 21(3):271–277.
[14] Oman SA, Ballinger L, Cerilli LA. Small cell carcinoma: arising in Lynch syndrome: a previously undocumented occurrence. Int J Surg Pathol, 2009, 17(1):46–50.
[15] Vergelí-Rojas JA, Santiago-Caraballo DL, Cáceres-Perkins W, Magno-Pagatzartundua P, Toro DH. Small cell neuroendocrine carcinoma of rectum with associated paraneoplastic syndrome: a case report. P R Health Sci J, 2013, 32(1):51–53.
[16] Kim ST, Lee SJ, Park SH, Park JO, Lim HY, Kang WK, Lee J, Park YS. Genomic profiling of metastatic gastroenteropancreatic neuroendocrine tumor (GEP-NET) patients in the personalized-medicine era. J Cancer, 2016, 7(9):1044–1048.
[17] Guida F, Clemente M, Valvano L, Napolitano C. Laparoscopic or open hemicolectomy for elderly patients with right colon cancer? A retrospective analysis. G Chir, 2015, 36(5):205–208.
[18] Basturk O, Yang Z, Tang LH, Hruban RH, Adsay V, McCall CM, Krasinskas AM, Jang KT, Frankel WL, Balci S, Sigel C, Klimstra DS. The high-grade (WHO G3) pancreatic neuroendocrine tumor category is morphologically and biologically heterogenous and includes both well differentiated and poorly differentiated neoplasms. Am J Surg Pathol, 2015, 39(5):683–690.
[19] Rekhtman N. Neuroendocrine tumors of the lung: an update. Arch Pathol Lab Med, 2010, 134(11):1628–1638.
[20] Acosta AM, Hamedani FS, Meeks JJ, Wu S. Primary ureteral thyroid transcription factor 1-positive small cell neuroendocrine carcinoma: case report and review of the literature. Int J Surg Pathol, 2015, 23(6):472–477.
[21] Hassan U, Mozayani B, Wong NA. Primary combined neuroendocrine carcinoma (small-cell type) and squamous cell carcinoma of the colon. Histopathology, 2016, 68(5):755–758.
[22] Meşină C, Vasile I, Ciobanu D, Calotă F, Gruia CL, Streba L, Mogoantă SŞ, Pârvănescu H, Georgescu CV, Tarniţă DN. Collision tumor of recto-sigmoidian junction – case presentation. Rom J Morphol Embryol, 2014, 55(2 Suppl):643–647.
[23] Liu XJ, Feng JS, Xiang WY, Kong B, Wang LM, Zeng JC, Liang YF. Clinicopathological features of an ascending colon mixed adenoneuroendocrine carcinoma with clinical serosal invasion. Int J Clin Exp Pathol, 2014, 7(9):6395–6398.
[24] Vanacker L, Smeets D, Hoorens A, Teugels E, Algaba R, Dehou MF, De Becker A, Lambrechts D, De Greve J. Mixed adenoneuroendocrine carcinoma of the colon: molecular pathogenesis and treatment. Anticancer Res, 2014, 34(10): 5517–5521.
[25] Lipka S, Hurtado-Cordovi J, Avezbakiyev B, Freedman L, Clark T, Rizvon K, Mustacchia P. Synchronous small cell neuroendocrine carcinoma and adenocarcinoma of the colon: a link for common stem cell origin? ACG Case Rep J, 2014, 1(2):96–99.
[26] Powell SM, Zilz N, Beazer-Barclay Y, Bryan TM, Hamilton SR, Thibodeau SN, Vogelstein B, Kinzler KW. APC mutations occur early during colorectal tumorigenesis. Nature, 1992, 359(6392):235–237.
[27] Miyoshi Y, Nagase H, Ando H, Horii A, Ichii S, Nakatsuru S, Aoki T, Miki Y, Mori T, Nakamura Y. Somatic mutations of the APC gene in colorectal tumors: mutation cluster region in the APC gene. Hum Mol Genet, 1992, 1(4):229–233.
[28] Giannakis M, Hodis E, Jasmine Mu X, Yamauchi M, Rosenbluh J, Cibulskis K, Saksena G, Lawrence MS, Qian ZR, Nishihara R, Van Allen EM, Hahn WC, Gabriel SB, Lander ES, Getz G, Ogino S, Fuchs CS, Garraway LA. RNF43 is frequently mutated in colorectal and endometrial cancers. Nat Genet, 2014, 46(12):1264–1266.
[29] Detweiler CJ, Cardona DM, Hsu DS, McCall SJ. Primary high-grade neuroendocrine carcinoma emerging from an adenomatous polyp in the setting of familial adenomatous polyposis. BMJ Case Rep, 2016, Feb 16, pii: bcr2015214206.
[30] Floquet C, Deforges J, Rousset JP, Bidou L. Rescue of nonsense mutated p53 tumor suppressor gene by aminoglycosides. Nucleic Acids Res, 2011, 39(8):3350–3362.
[31] Kemp Z, Rowan A, Chambers W, Wortham N, Halford S, Sieber O, Mortensen N, von Herbay A, Gunther T, Ilyas M, Tomlinson I. CDC4 mutations occur in a subset of colorectal cancers but are not predicted to cause loss of function and are not associated with chromosomal instability. Cancer Res, 2005, 65(24):11361–11366.
[32] Li N, Lorenzi F, Kalakouti E, Normatova M, Babaei-Jadidi R, Tomlinson I, Nateri AS. FBXW7-mutated colorectal cancer cells exhibit aberrant expression of phosphorylated-p53 at Serine-15. Oncotarget, 2015, 6(11):9240–9256.
[33] Uchino S, Noguchi S, Yamashita H, Sato M, Adachi M, Yamashita H, Watanabe S, Ohshima A, Mitsuyama S, Iwashita T, Takahashi M. Somatic mutations in RET exons 12 and 15 in sporadic medullary thyroid carcinomas: different spectrum of mutations in sporadic type from hereditary type. Jpn J Cancer Res, 1999, 90(11):1231–1237.
[34] Dixit A, Torkamani A, Schork NJ, Verkhivker G. Computational modeling of structurally conserved cancer mutations in the RET and MET kinases: the impact on protein structure, dynamics, and stability. Biophys J, 2009, 96(3):858–874.
[35] Li YY, Hanna GJ, Laga AC, Haddad RI, Lorch JH, Hammerman PS. Genomic analysis of metastatic cutaneous squamous cell carcinoma. Clin Cancer Res, 2015, 21(6):1447–1456.
[36] Mouradov D, Sloggett C, Jorissen RN, Love CG, Li S, Burgess AW, Arango D, Strausberg RL, Buchanan D, Wormald S, O'Connor L, Wilding JL, Bicknell D, Tomlinson IP, Bodmer WF, Mariadason JM, Sieber OM. Colorectal cancer cell lines are representative models of the main molecular subtypes of primary cancer. Cancer Res, 2014, 74(12):3238–3247.

Corresponding author
Andrzej Wincewicz, MD, Fellow of European Board of Pathology (FEBP), Specialist Medical Practice – Pathologist, Non Public Health Care Unit, Department of Pathology (NZOZ Zakład Patologii Spółka z o.o.), ul. Jagiellońska 70, 25–734 Kielce, Poland; Phone +48 41 368 47 87, Fax +48 41 366 17 81, e-mails: ruahpolin@yahoo.com, andwinc@gmail.com

Received: December 21, 2016 *Accepted: July 14, 2017*